HHS Public Access

Author manuscript

J Chromatogr A. Author manuscript; available in PMC 2022 April 13.

Published in final edited form as:

J Chromatogr A. 2021 June 21; 1647: 462144. doi:10.1016/j.chroma.2021.462144.

Ionic liquid stationary phase coating optimization for semi-packed microfabricated columns

Azam Gholizadeh, **Mustahsin Chowdhury**, **Masoud Agah***

VT MEMS Lab, Bradley Department of Electrical and Computer Engineering, Virginia Tech, Blacksburg, VA, 24061, United States

Abstract

This work highlights the effect of the stationary phase coating process on the separation efficiency of gas chromatography microcolumns. The stationary phase coating quality was characterized by three different bis(trifluoromethylsulfonyl)imide (NTf_2) anion based ionic liquids. The ionic liquids containing NTf_2 anion are used for gas chromatography due to their high temperature stability. In this work, the chemical and physical approaches of column deactivation as well as the temperature treatment were evaluated by separating a mixture of 20 organic components and saturated alkanes. The results show that higher oven temperature treatment provides higher efficiency while losing a bit of peak symmetry. The thermal treated 1-butylpyridinum bis(trifluoromethylsulfonyl) imide [BPY][NTf_2] stationary phase at 240°C demonstrated as high as 8300 plates per meter for naphthalene. This was a 5-fold increase in separation efficiency in comparison to those of the columns treated at 200°C. Albeit being within acceptable ranges, the peak tailing degraded from 1.17 to 1.46 for naphthalene when the processing temperature for coating increased. Both chemical and physical deactivation process increased separation efficiencies and peak resolution.

Keywords

Gas chromatography; Semi-packed microcolumn; Ionic liquids; Stationary phase coating

*Corresponding author at: Masoud Agah - VT MEMS Lab, Bradley Department of Electrical and Computer Engineering, Virginia Tech, Blacksburg, VA, 24061, United States. agah@vt.edu (M. Agah).

Declaration of Competing Interest

The authors declare no competing financial interest.

CRediT authorship contribution statement

Azam Gholizadeh: Conceptualization, Investigation, Formal analysis, Methodology, Writing – original draft, Software. **Mustahsin Chowdhury:** Conceptualization, Investigation, Writing – review & editing, Visualization. **Masoud Agah:** Conceptualization, Methodology, Supervision, Writing – review & editing, Project administration.

Supplementary materials

Supplementary material associated with this article can be found, in the online version, at doi:10.1016/j.chroma.2021.462144.

Appendix A. Supporting Information

Supporting information includes the effect of temperature ramp on chromatograms of saturated alkanes, the effect of repeating runs and cleaning steps on the response of columns towards naphthalene, and list of chemicals in 20 components mixture.

1. Introduction

Separation performance achieved by gas chromatography (GC) depends on several important factors, such as the column dimensions, the type of the stationary phase, and the operational conditions, including column temperature and flow velocity. Among these factors, the stationary phase coating process is crucial and can significantly influence the separation efficiency under the same column dimensions and operating conditions.

Polydimethyl siloxane (PDMS), phenyl-methylpolysiloxane, cyanopropylphenyl-methylpolysiloxane, and polyethylene glycol [1-3] are among some typical stationary phases used in GCs. However, these traditional stationary phases are susceptible to moisture and oxygen, which subsequently can lead to column bleeding. They also have limited thermal stability and do not provide flexibility to modify their chemical structure to enhance or program separation selectivity [4]. Ionic liquids (ILs) have attracted attention as a new class of stationary phases to address some of these deficiencies. ILs were introduced as a GC stationary phase candidates in 1982 by applying the ethyl ammonium nitrate as the stationary phase. The proposed stationary phase successfully separated a wide range of volatile organic compounds at temperatures below 120 °C. Other groups prepared GC columns based on tetraalkylphosphonium salts, but they produced poor efficiency [5, 6]. Ethylpyridinium bromide and imidazolium based ILs were the first promising stationary phases that exhibited similar efficiencies to conventional stationary phases [7, 8]. Later studies indicated the high efficiency achievable by NTf_2 anion especially for alcohols and aromatic isomers [9].

ILs are good candidates for GC phases because they are stable at high temperatures. They are viscous enough to enable them to move easily through the column during the coating process, and they provide high separation efficiency [8, 10]. The unique properties of ILs result from the fact that they are entirely imposed of ions that can be easily changed. Theoretically, there are infinite possibilities to change and program their chemical structures to enhance selectivity toward target compounds [11]. The more exciting aspect of ILs is that they demonstrate unusual dual nature retention behavior, separating both polar and nonpolar chemicals. The dual separation capability is possible because of their various intermolecular interaction capabilities. They apply their dispersion interaction capabilities to separate nonpolar molecules. Besides, they can use dipolar, charge interactions, and hydrogen bonding to separate polar compounds [12].

Several different ILs have been applied as stationary phases in GC and multidimensional GC. The most common ILs based stationary phases are monocationic ones. They can be a combination of cations such as ammonium, sulfonium, imidazolium, and pyridinium and anions of halide, tetrafluoroborate [BF_4], triflate [TfO], hexafluorophosphate [PF_6], and [NTF_2]. Later, Di and Polycationic ILs were also introduced that demonstrated significantly higher thermal stability compared to monocationic ILs. Furthermore, polymeric ILs were shown even higher thermal stability. The results indicated that step growth method to produce polymeric ILs is more efficient than chain growth to enhance thermal stability of the stationary phase. Metal containing ILs as another branch of the ILs stationary phase, were highly selective towards hydrocarbons of various sizes. Besides, Armstrong and co-workers

introduced water-compatible IL based stationary phases that now commercially available. These stationary phase based columns can be used for the direct analysis of samples with water as the solvent, making them very important for the analysis of environmental and biological samples. Also, the lack of inertness of ILs was overcame using inert Ils such as SLB-IL60i, SLBIL76i that were introduced by Millipore Sigma in 2016 [13].

The proper coating process is required to apply these unique properties of ILs into the GC system. There are two different coating techniques for GC columns, including those utilized for columns fabricated using the microelectromechanical systems (MEMS) technology: dynamic and static [14]. In the dynamic mode, the stationary phase solution slowly moves through the column by applying a differential gas pressure along the column length. The film thickness in this method depends on the plug velocity and the initial stationary phase concentration. The dynamic coating usually produces non-uniform film thickness due to axial motion, potentially decreasing the column efficiency. High gas pressures may also promote the coating solution's flashing and leave devoid areas on the surface of the column walls [15]. The static coating technique involves the loading of the column with the stationary phase solution. Once the column is filled, the solvent is evaporated using vacuum at a constant temperature [16].

MEMS columns offer fast analysis time with less thermal mass allowing rapid temperature programming with low power consumption. These attributes make these columns attractive for the applications involving on-site monitoring of volatile organic compounds (VOCs) in complex samples [17, 18]. Achieving a consistent stationary phase in MEMS columns is more challenging due to liquid pooling in the corners of microchannels and complex fluid dynamic behavior inside the MEMS columns [19]. Different stationary phases and coating strategies have been utilized for the functionalization of MEMS columns. PDMS and WAX have been employed to separate nonpolar and polar mixtures (such as fatty acids and alcohols), respectively [20-22]. Dynamic coating of PDMS as a typical nonpolar phase has shown 20 0 0 to 2500 theoretical plates per meter [23-25]. In another work, a square-spiral 3-m column of the microfabricated GC analyzers was dynamically coated with PDMS [25]. The stationary phase thickness was estimated to be 1-2 μm, and up to 8200 theoretical plates number was obtained [26]. Another stationary phases used in both capillary tubing and MEMS columns are nanomaterials such as carbon nanotubes and gold nanoparticles [27]. Several other phases are also proposed, such as metal-organic compounds [28], alumina [29], sputtered oxide, graphite [30, 31], and silica nanoparticles [32]. As ionic liquids demonstrated promising results in conventional columns, they were introduced as a stationary phase for the MEMS semi-packed columns by our group which exhibited high performance separation efficiencies and good resolution [33, 34].

The goal of this research is to introduce fast coating method and study the effect of the coating steps on the performance of the semi-packed MEMS columns. It was evaluated using three ILs stationary phases that we introduced in our previous work [35]. In this paper, we also investigate the effect of the deactivation process on the performance of the MEMS columns. The effect of physical deactivation using the atomic layer deposited alumina was compared with a fast chemical silanization reaction. The separation performance was investigated using 20 organic components mixture and saturated alkanes.

2. Materials and Methods

2.1. Materials

Three RTILs, namely, 1-butylpyridinum bis(trifluoromethylsul fonyl)imide ([BPY][NTf_2] (IL1), Methyltrioctylammonium bis (trifluoromethylsulfonyl)imide [N1888][NTf_2] (IL2) and 1-(2-Hydroxyethyl)-3-methylimidazolium bis(trifluoromethylsulfonyl) imide [HOEMIM][NTf_2] (IL3) were obtained from Ionic Liquids Technologies, Inc. (Tuscaloosa, AL, US). Silicon wafers (n-typed, 4 in diameter, 500 μm thickness, double sided polished) and Borofloat wafer (4 in diameter, 175 μm thickness) were purchased from University Wafer, Inc. (Boston, MA, US). Fused silica capillary tubes with 100 μm internal diameter and 200 μm outer diameter were purchased from Polymicro Technologies, LLC. (Lisle, IL, US). Fused capillary tube with 15 m length and 0.25 mm thickness, Capillary column with 15 m length and 0.25 mm thickness were purchased from Restek (Bellefonte, PA, US). JB Weld epoxy was obtained from the local store. Dimethyl ethyl silane, tris (pentafluorophenyl)borane, acetone, naphthalene, heptane, octane, nonane, benzene, toluene, ethylbenzene, p-Xylene, m-Xylene, o-Xylene, isobutylbenzene, styrene, butylbenzene, 1,2-Dichlorobenzene, 2,5-Dichlorotoluene, 1,2,4-Trichlorobenzene, benzyl chloride, 2-nitrotoluene, 3-nitrotoluene, 4-nitrotoluene, and standard of C7-C30 saturated alkanes (1000 μg/ml each compound in hexane) were purchased from Sigma Aldrich (St Louis, MO, US). Ultrapure helium, nitrogen, hydrogen, and air were obtained from Airgas, Inc. (Christiansburg, VA, US). Table 1 shows the order of retention times and temperature of ebullition for the 20 components. All solutions were kept in the refrigerator before using them. The retention time of individual chemicals was achieved separately.

2.2. Instrumentation

All gas chromatography measurements used to characterize the behavior of the ionic liquids were performed on an Agilent 7890A GC (Agilent Technologies, Inc, Santa Clara, CA, US) system equipped with an automatic sampler (7693A), split/splitless inlet, and flame ionization detector (FID). Helium was used as a mobile phase. The flow rate of hydrogen and air for FID detector were kept at 30 ml/min and 300 ml/min, respectively. SEM images were obtained using Carl (Zeiss) EVO 40 Scanning Electron Microscope (SEM). The data were analyzed using the Agilent ChemStation Edition C.01.04.

2.3. Column fabrication

The detail of the fabrication of the semi-packed columns was discussed in our previous reports [34, 35]. Briefly, the etching photoresist mask was pattern on surface of the silicon wafer using AZ9260 photoresist. Then silicon pillars were created using deep reactive ion etching (DRIE) process. Sulfur hexafluoride (SF6) and octafluorocyclobutane were used in the etchant and passivation steps. The etched pillar were the circular with around 20 μm in diameter with depth of 240 μm and column length of 1 m. After removing photoresist mask using acetone, piranha, and oxygen plasma, the etched silicon wafer was anodically bonded with a 175 μm thick Borofloat glass wafer at 1250 V and 400°C. After dicing the wafer into the individual microcolumns, the inlet and outlet were attached to 30 cm long silica capillary tubing. Stationary phase coating was performed using a freshly prepared solution

with a concentration of 15 mg/ml in acetone for IL1, IL2, and 1.5 mg/ml in acetone for IL3 stationary phases.

3. Results and Discussion

3.1. Coating method

Columns deactivation is the first step before starting the stationary phase coating process. Physical deactivation was achieved by depositing 13 nm of an aluminum oxide layer using atomic layer deposition (ALD) [29]. However, chemically deactivating silicon-based GC columns is typically used to enhance their efficiency. The most common chemical method used for this purpose involves the reaction between silanol groups (Si-OH) present on the surface of silicon and organosilicon compounds, such as dimethylaminosilanes, chlorosilanes, alkoxysilanes, and allylsilanes [36-39]. Despite the wide application of these approaches, undesirable polysiloxane networks are often created. These methods require long reaction times between 2-24 h. In this paper, the column efficiency was enhanced by using a fast chemical silanization reaction (Fig. S1). The chemical deactivation was performed with creating an organic monolayer by siloxanation of oxidized silicon pillars surfaces. The 1% dimethyl ethyl silane and tris (pentafluorophenyl)borane ($B(C_6F_5)_3$) as a catalyst were prepared in CH_2Cl_2 and injected inside the column with a flow rate of 20 μl/min. The supplementary video clip 1 shows the process. The bubbles seem in the video are related to the hydrogen generation during chemical deactivation. Following this step, the column was washed with CH_2Cl_2 for 30 minutes until no bubbles were detectable inside the column. This method is one of the fastest GC column deactivation process that the salinization reaction only takes a few minutes to accomplish [39, 40].

To achieve a mass produce of uniform stationary phase coating, designing a fast coating procedure free of bubbles is crucial. Fig. 1 indicates the schematic of the optimum coating steps. Several coating and drying strategies were investigated to achieve an efficient method. Fig. 2 shows the microcolumns filled with IL solution using the N_2 purging method (commonly used approach by our group and others) and the syringe pump. Using N_2 for solution purging leaves behind bubbles especially at the end parts of the column and the curved regions (Fig. 2A). Applying a constant flow rate with a syringe pump gives a chance to fill the ionic liquid solution uniformly (supplementary video clip 2). After the column packed with the solution, the flow rate was increased to cover up any remaining empty spots (supplementary video clip 3). Fig. 2B demonstrates smooth and bubble-free coated microcolumns using 20, 40, and 60 μl/min of the solution flow rates. In the next step of the coating, the solvent is required to evaporate and leave behind the thin layer of the stationary phase on the surfaces of the entire column. Different strategies were applied to dry the column. Fig. 2 provides the effect of them on the smoothness of the drying procedure. In one method, the withdraw mode of the syringe pump was used to create a local vacuum and push back the extra solution from the column. The process was examined in both sealed and open-ended situations. In both cases, nonuniform residues of the solution were observed inside the channels (Fig. 2C). In another technique, N_2 purging was used to accelerate the evaporation process. Still, the nonuniform residues were created (Fig. 2D). Finally, the N_2 purging was combined with a water bath (Fig. 2E). This process accomplished the drying

procedure in less than 10 minutes. Fig. 2F shows after one minute N_2 purging, while Fig. 2G shows a uniformly dried column after four minutes. The column was kept for a while to make sure solvent residues escaped from the channels. Elevated uniform temperature using a water bath with a combination of N_2 flow provides fast and uniform removal of excess coating solution and avoids trapping microbubbles between silicon pillars. All these three procedures gave better drying quality than using an overnight vacuum inside a desiccator. So, the N_2 purging with a water bath of 40°C was selected through the entire work as the preferred drying step.

Fig. 3A shows the column after coating with a syringe pump and drying using N_2 purging in the water bath. The inset of the figure indicates SEM images of the four pillars silicon array. The SEM was used to monitor the smoothness and thickness of the IL stationary phase of the GC microcolumns. Fig. 3B shows the ionic liquid around the silicon pillars. It can be seen that with the selected coating method, the uniform layer of the ionic liquid was created around the silicon pillars. Inset demonstrated the magnified image of the stationary phase layer. The upper observed distortion happened during the peeling out of the upper layer to prepare for the SEM image. Figs. 3C and 3D indicate the optical microscope images of the column before and after the oven pretreatment. The column's treatment in 240 °C removes all solvent residues on the glass slide and around the pillars and stabilizes the ionic liquid layer.

3.2. Chromatographic characterization of the coated microcolumns

To characterize the quality of the column coating, column efficiency and column resolution were investigated. The efficiency of a column is reported as the height-equivalent-to-a-theoretical-plate (HETP) that is inversely related to the number of theoretical plates. The resolution denotes how the two adjacent peaks are separated. The geometry of the column and the thickness of the stationary phase play important roles in the column performance. Naphthalene was used as a probe to calculate plate number as it is well retained compound and was used in many studies to evaluate the column efficiency [33]. Naphthalene was injected into the columns under isothermal temperature (100 °C) to obtain the corresponding HETP values. The trend line between the HETP and the carrier gas velocity is shown in Fig. 4. It represents the effect of ionic liquid type, deactivation method, and coating thermal pretreatment temperature on the efficiency of the microcolumns. Fig. 4A indicates the effect of the pretreatment temperature on the efficiency of IL1. The three different temperatures of 200 °C, 220 °C, and 240 °C were applied. HETP for IL1 column treated at 240 °C is lower within a broader range of the carrier gas velocity. The 240 °C treated IL2 shows lower HETP at any given carrier gas velocity. Besides, IL2 demonstrates similar thermal treatment behavior to IL1. In addition to the thermal treatment, the effect of IL's type was investigated (Fig. 4B). Different ionic liquids present different trajectories; IL3 treated at 200 °C shows lower HETP when compared to that of IL2 treated at 220 °C. Fig. 4C represents the effect of the deactivation methods of the silicon surface. Both chemical and physical deactivated columns show lower HETP and better efficiency compared to the non-deactivated column. While ALD surface treatment shows better efficiency, it may not be accessible in some nanofabrication facilities. The results show that the proposed chemical deactivation process can produce comparable results, especially in lower carrier gas velocities. The measurement

was repeated for two columns, and an average variation of 400 was found between columns (R^2=0.99) (Fig. 4D).

The efficiency of the semipacked column coated with ILs was compared with the commercial capillary column with 15 m length and 0.25 mm thickness coated with BP20 as the stationary phase and the same capillary column coated with IL1. Fig. S2 shows the HETP of the capillary columns. Semipacked column with a similar stationary phase compared to the capillary column demonstrates holding efficiency in higher carrier gas velocity making it possible to analyze the analytes in shorter times with the appropriate resolution values.

A plot of the theoretical plate height versus carrier gas velocity will never become completely linear and is different for various GC column types. In literature for the packed column, efficiency is represented by the van Deemter (equation 1).

$$\mathrm{HETP} = A + (B / x) + Cx \tag{1}$$

Where A is the eddy diffusion results because in packed columns spaces between particles along the column are not uniform. Therefore, molecules take different pathways along the column, B is the coefficient for longitudinal diffusion, and C is the resistance to mass transport in the gas and liquid phases, and x is the carrier gas velocity.

For square spiral semipacked columns, Golay-Goucheon kinetic model was shown better regression fit in previous works (equation 2).

$$\mathrm{HETP} = (B / x) + Cx + Dx^2 \tag{2}$$

Where D was defined as the extracolumn band broadening [23, 41]. For the semipacked silicon pillar that was reported in this work, both these equations did not provide perfect fitness. We figured out the combination of them shows the best fit for the experimental Golay plot represented in Fig. 4. Fig. S3 shows the amount of fitness for different Golay equations for one of the cases of IL stationary phases. Based on data, equation 3 was used to calculate Golay coefficients.

$$\mathrm{HETP} = A + (B / x) + Cx + Dx^2 \tag{3}$$

This seems reasonable as silicon pillars can create different pathways similar to the particles in the packed column, so eddy diffusion should also be considered. Table 2 represents the calculated values for A, B, C, and D for different kinds of ionic liquid stationary phases. Data shows higher efficient columns indicate lower eddy and longitude diffusion coefficients and have lower mass transfer resistance.

The separation performance of the MEMS columns was evaluated using a sample mixture, including 20 compounds with the boiling point in the range of 80 °C to 238 °C. The separation of the saturated alkanes was examined for the IL1 stationary phase under different

coating and different temperature ramp conditions (Figs. S4, S5). The performance of the columns' coating was evaluated with temperature-programmed chromatograms. Fig. 5 shows chromatograms of the MEMS columns with the IL1 stationary phase treated at 200 °C (A), 220 °C (B), and 240 °C (C) oven temperatures. The starting temperature was 30 °C, and the programming rate was 40 °C/min. As the data demonstrates, the oven temperature treatment dramatically influences the efficiency and the peak symmetry of the IL stationary phases based columns. The plate number of the IL1 columns increased from 1600 at 20 psi (200 °C) to 8300 at 45 psi (240 °C) with increasing the treatment temperature. Besides, it affects the symmetry and the resolution of the peaks. Table 3 shows the tailing factor and the resolution of naphthalene (1), 2-nitrotoluene (2), 3-nitrotoluene, and 4-nitrotoluene (4) peaks. The resolution values refer to the resolution between the peak of interest and the preceding peak. Similar to the plate number, the resolution increases with the treatment temperature. Despite some increase in peak tailing, all values are below 2. Also, the Retention factor (k) of naphthalene was found 11.5 for IL1, 4 for IL2 at an inlet pressure of 45 psi, and 7.8 for IL3 at an inlet pressure of 35 psi.

The same pattern of the plate number and resolution was observed for the IL2 stationary phase columns (Fig. 6). Fig. 6A shows the mixture separation using IL3 stationary phase treated at 200 °C. The elution times for some chemicals have been changed compared to IL1, suggesting the different selectivity provided by ILs for these compounds. Among all prepared columns, IL3 can separate p-Xylene from m-Xylene (peak numbers 7 and 8). Figs. 6B and 6C show the chromatograms for IL2 thermally treated at 220 °C and 240 °C. Our data also indicate the crucial role of the thermal treatment in enhancing the plate numbers. The measured plate numbers were 3000 at 35 psi for the IL2 column before the treatment. After treatment at 240 °C, the plate number increased to 7800 at 35 psi. Table 4 shows the resolution and tailing analysis for IL2 and IL3 columns. With a similar trend for IL1, for these columns, the resolution also improved by increasing the treatment temperature. The increasing trend for efficiency and resolution can be related to the ionic liquids' thermal dependence of viscosity. Previous researches indicated that decreasing viscosity of ionic liquids with increasing thermal treatment. Lower viscosity can lower mass transfer resistance and improve the interaction between the gas molecules with ionic liquid based stationary phases [42, 43].

Fig. 7 shows the chromatogram of the columns (A) compared with the chemically deactivated columns with dimethyl ethyl silane in the presence of the tris (pentafluorophenyl)borane as a catalyst (B). The deactivation improved the symmetry and the resolution of the peaks. This improvement comes from the deactivation of the active chemical sites on the surface of the silicon, such as hydroxyl and silica groups.

The presented preliminary data regarding this fast deactivation method is promising. However, more studies are required to investigate the effect of other types of silanes on the separation efficiency.

Besides, the performance of the semipacked column was compared with 15 m capillary columns. Figs. S6, S7 show the chromatograms of 20 components that were used to evaluate the semi-packed columns. The data was achieved in 45 psi to compare with semipacked

columns. Moreover, as the capillary columns had the best efficiency at 10 psi carrier gas pressure, corresponding data were also reported. Tables S1 and S2 demonstrate the resolution and symmetry data for the three last peaks in the chromatograms. The resolution was reported between peak of interest and the preceding peak, and symmetry was reported based on tailing at 5% height of the peaks. At the same carrier gas pressure of 45 psi, the capillary column based on IL1 shows a more symmetric peak but lower resolution than the IL1 based semipacked column. In contrast, the capillary column based on BP20 demonstrates better resolution and symmetry in comparison to the semipacked columns.

The stability of the IL-based MEMS columns was also investigated for 100 repeated runs. The data was obtained for naphthalene under 30 psi carrier gas pressure with 0.3 μL injection of sample. For all ILs, there is a significant difference between the first and the second run, but it stabilizes after the second run. Results show height is the most affected variable. Besides, based on relative standard deviation (RSD) data, IL1 with 2.11 height RSD in comparison to 4.47 and 4.50 for IL2 and IL3, respectively, is a more stable column (Table 5). The effect of cleaning between each run also was investigated. More detailed data have been provided in the supplementary section (Figs. S8, S9).

4. Conclusion

The importance of the coating method for ionic liquid stationary phase MEMS columns was evaluated in this study. The results herein proved that the coating and drying steps play important roles in the uniformity of the stationary phase. Optimized thermal treatment can dramatically enhance the efficiency of the columns. The modified static coating described here indicated better performance when using a syringe pump with well-controlled multiple flow rates procedure, N_2 purging combined with water bath as a drying step, and thermal treatment in the oven as a stabilizing step. Furthermore, the fast chemical deactivation method introduced in this work can facilitate the fabrication of the MEMS columns for certain applications. The information was provided here would be useful for designing an optimized, fast and reliable coating method for stationary phases for microfabricated separation columns. In line with our recent publications, the data also reaffirms the usability of ILs as reliable stationary phases for MEMS columns in general and our semi-packed columns in particular.

Supplementary Material

Refer to Web version on PubMed Central for supplementary material.

Acknowledgments

The work has been supported by the National Institute of Occupational Safety and Health (NIOSH) under the award number R01OH011350. The columns were fabricated at Virginia Tech’s Micron Semiconductor Fabrication. Laboratory. SEM images were taken at College of Veterinary Medicine at Virginia Tech.

References

[1]. Menestrina F, Ronco NR, Romero LM, Castells CB, Enantioseparation of polar pesticides on chiral capillary columns based on permethyl-β-cyclodextrin in matrices of different polarities, Microchemical Journal 140 (2018) 52–59.

[2]. Mayer BX, Zöllner P, Lorbeer E, Rauter W, A new 75% diphenyl, 25% dimethyl-polysiloxane coated on fused silica capillary columns for high temperature gas chromatography, Journal of separation science 25 (2002) 60–66.

[3]. Poole CF, Poole SK, Ionic liquid stationary phases for gas chromatography, Journal of separation science 34 (2011) 888–900. [PubMed: 21290604]

[4]. Rahman MM, Abd El-Aty A, Choi JH, Shin HC, Shin SC, Shim JH, Basic overview on gas chromatography columns, Analytical Separation Science (2015) 823–834.

[5]. Pacholec F, Butler HT, Poole CF, Molten organic salt phase for gas-liquid chromatography, Analytical Chemistry 54 (1982) 1938–1941.

[6]. Pomaville RM, Poole SK, Davis LJ, Poole CF, Solute—solvent interactions in tetra-n-butylphosphonium salts studied by gas chromatography, Journal of Chromatography A 438 (1988) 1–14.

[7]. Pacholec F, Poole C, Stationary phase properties of the organic molten salt ethylpyridinium bromide in gas chromatography, Chromatographia 17 (1983) 370–374.

[8]. Armstrong DW, He L, Liu Y-S, Examination of ionic liquids and their interaction with molecules, when used as stationary phases in gas chromatography, Analytical chemistry 71 (1999) 3873–3876. [PubMed: 10489532]

[9]. Hsieh Y-N, Ho W-Y, Horng RS, Huang P-C, Hsu C-Y, Huang H-H, et al. , Study of anion effects on separation phenomenon for the vinyloctylimidazolium based ionic liquid polymer stationary phases in GC, Chromatographia 66 (2007) 607–611.

[10]. Anderson JL, Ding J, Welton T, Armstrong DW, Characterizing ionic liquids on the basis of multiple solvation interactions, Journal of the American Chemical Society 124 (2002) 14247–14254. [PubMed: 12440924]

[11]. Soukup-Hein RJ, Warnke MM, Armstrong DW, Ionic liquids in analytical chemistry, Annual Review of Analytical Chemistry 2 (2009) 145–168.

[12]. Anderson JL, Armstrong DW, Wei G-T, Ionic liquids in analytical chemistry, ACS Publications, 2006.

[13]. Trujillo-Rodríguez MJ, Nan H, Varona M, Emaus MN, Souza ID, Anderson JL, Advances of ionic liquids in analytical chemistry, Analytical chemistry 91 (2018) 505–531. [PubMed: 30335970]

[14]. Grob K, in: Making and Manipulating Capillary ColumnsforGas Chromatography, Hüthig, Heidelberg, 1986, p. 36.

[15]. Scott RP, Principles and practice of chromatography, 1, Chrom-ed book series, 2003.

[16]. Currie RW, Christiansen D, Gas chromatography capillary devices and methods, Google Patents, 2012.

[17]. Bhushan A, Yemane D, Trudell D, Overton EB, Goettert J, Fabrication of micro-gas chromatograph columns for fast chromatography, Microsystem Technologies 13 (2007) 361–368.

[18]. Reidy S, George D, Agah M, Sacks R, Temperature-programmed GC using silicon microfabricated columns with integrated heaters and temperature sensors, Analytical chemistry 79 (2007) 2911–2917. [PubMed: 17311465]

[19]. Sumpter SR, Lee ML, Enhanced radial dispersion in open tubular column chromatography, Journal of Microcolumn Separations 3 (1991) 91–113.

[20]. Sun J, Cui D, Li Y, Zhang L, Chen J, Li H, et al. , A high resolution MEMS based gas chromatography column for the analysis of benzene and toluene gaseous mixtures, Sensors and Actuators B: Chemical 141 (2009) 431–435.

[21]. Ali S, Ashraf-Khorassani M, Taylor LT, Agah M, MEMS-based semi-packed gas chromatography columns, Sensors and Actuators B: Chemical 141 (2009) 309–315.

[22]. Chen B-X, Hung T-Y, Jian R-S, Lu C-J, A multidimensional micro gas chromatograph employing a parallel separation multi-column chip and stop-flow μGC× μGCs configuration, Lab on a Chip 13 (2013) 1333–1341. [PubMed: 23381092]

[23]. Lambertus G, Elstro A, Sensenig K, Potkay J, Agah M, Scheuering S, et al. , Design, fabrication, and evaluation of microfabricated columns for gas chromatography, Analytical chemistry 76 (2004) 2629–2637. [PubMed: 15117208]

[24]. Lambertus G, Sacks R, Stop-flow programmable selectivity with a dual-column ensemble of microfabricated etched silicon columns and air as carrier gas, Analytical chemistry 77 (2005) 2078–2084. [PubMed: 15801741]

[25]. Lambertus GR, Fix CS, Reidy SM, Miller RA, Wheeler D, Nazarov E, et al. , Silicon microfabricated column with microfabricated differential mobility spectrometer for GC analysis of volatile organic compounds, Analytical Chemistry 77 (2005) 7563–7571. [PubMed: 16316163]

[26]. Azzouz I, Vial J, Thiébaut D, Haudebourg R, Danaie K, Sassiat P, et al. , Review of stationary phases for microelectromechanical systems in gas chromatography: feasibility and separations, Analytical and bioanalytical chemistry 406 (2014) 981–994. [PubMed: 23929190]

[27]. Stadermann M, McBrady AD, Dick B, Reid VR, Noy A, Synovec RE, et al. , Ultrafast gas chromatography on single-wall carbon nanotube stationary phases in microfabricated channels, Analytical chemistry 78 (2006) 5639–5644. [PubMed: 16906706]

[28]. Read D, Sillerud CH, Metal-Organic Framework Thin Films as Stationary Phases in Microfabricated Gas-Chromatography Columns, Sandia National Laboratories (SNLNM), Albuquerque, NM (United States), 2016.

[29]. Shakeel H, Rice GW, Agah M, Semipacked columns with atomic layer-deposited alumina as a stationary phase, Sensors and Actuators B: Chemical 203 (2014) 641–646.

[30]. Vial J, Thiébaut D, Marty F, Guibal P, Haudebourg R, Nachef K, et al. , Silica sputtering as a novel collective stationary phase deposition for microelectromechanical system gas chromatography column: Feasibility and first separations, Journal of Chromatography A 1218 (2011) 3262–3266. [PubMed: 21208620]

[31]. Haudebourg R, Vial J, Thiebaut D, Danaie K, Breviere J, Sassiat P, et al. , Temperature-programmed sputtered micromachined gas chromatography columns: An approach to fast separations in oilfield applications, Analytical chemistry 85 (2013) 114–120. [PubMed: 23231068]

[32]. Wang D, Shakeel H, Lovette J, Rice GW, Heflin JR, Agah M, Highly stable surface functionalization of microgas chromatography columns using layer-by-layer self-assembly of silica nanoparticles, Analytical chemistry 85 (2013) 8135–8141. [PubMed: 23889461]

[33]. Regmi BP, Chan R, Agah M, Ionic liquid functionalization of semi-packed columns for high-performance gas chromatographic separations, Journal of Chromatography A 1510 (2017) 66–72. [PubMed: 28662852]

[34]. Regmi BP, Chan R, Atta A, Agah M, Ionic liquid-coated alumina-pretreated micro gas chromatography columns for high-efficient separations, Journal of Chromatography A 1566 (2018) 124–134. [PubMed: 30017088]

[35]. Gholizadeh Azam CM, Masoud Agah, Analytiocal Chemistry (2021) (Online early access).

[36]. Dugas V, Chevalier Y, Chemical Reactions in Dense Monolayers: In situ thermal cleavage of grafted esters for preparation of solid surfaces functionalized with carboxylic acids, Langmuir 27 (2011) 14188–14200. [PubMed: 22026445]

[37]. Pasternack RM, Rivillon Amy S, Chabal YJ, Attachment of 3-(aminopropyl) triethoxysilane on silicon oxide surfaces: dependence on solution temperature, Langmuir 24 (2008) 12963–12971. [PubMed: 18942864]

[38]. Park J-W, Jun C-H, Transition-metal-catalyzed immobilization of organic functional groups onto solid supports through vinylsilane coupling reactions, Journal of the American Chemical Society 132 (2010) 7268–7269. [PubMed: 20450159]

[39]. Yuan H, Du X, Tai H, Li Y, Zhao X, Guo P, et al. , The effect of the channel curve on the performance of micromachined gas chromatography column, Sensors and Actuators B: Chemical 239 (2017) 304–310.

[40]. Radadia AD, Masel RI, Shannon MA, Jerrell JP, Cadwallader KR, Micromachined GC columns for fast separation of organophosphonate and organosulfur compounds, Analytical Chemistry 80 (2008) 4087–4094. [PubMed: 18442266]

[41]. Giddings JC, Liquid distribution on gas chromatographic support. Relationship to plate height, Analytical Chemistry 34 (1962) 458–465.

[42]. Omotowa BA, Phillips BS, Zabinski JS, Shreeve J.n.M., Phosphazene-based ionic liquids: synthesis, temperature-dependent viscosity, and effect as additives in water lubrication of silicon nitride ceramics, Inorganic chemistry 43 (2004) 5466–5471. [PubMed: 15310229]

[43]. Ciocirlan O, Iulian O, Croitoru O, Effect of temperature on the physico-chemical properties of three ionic liquids containing choline chloride, Rev Chim (Bucharest) 61 (2010) 721–723.

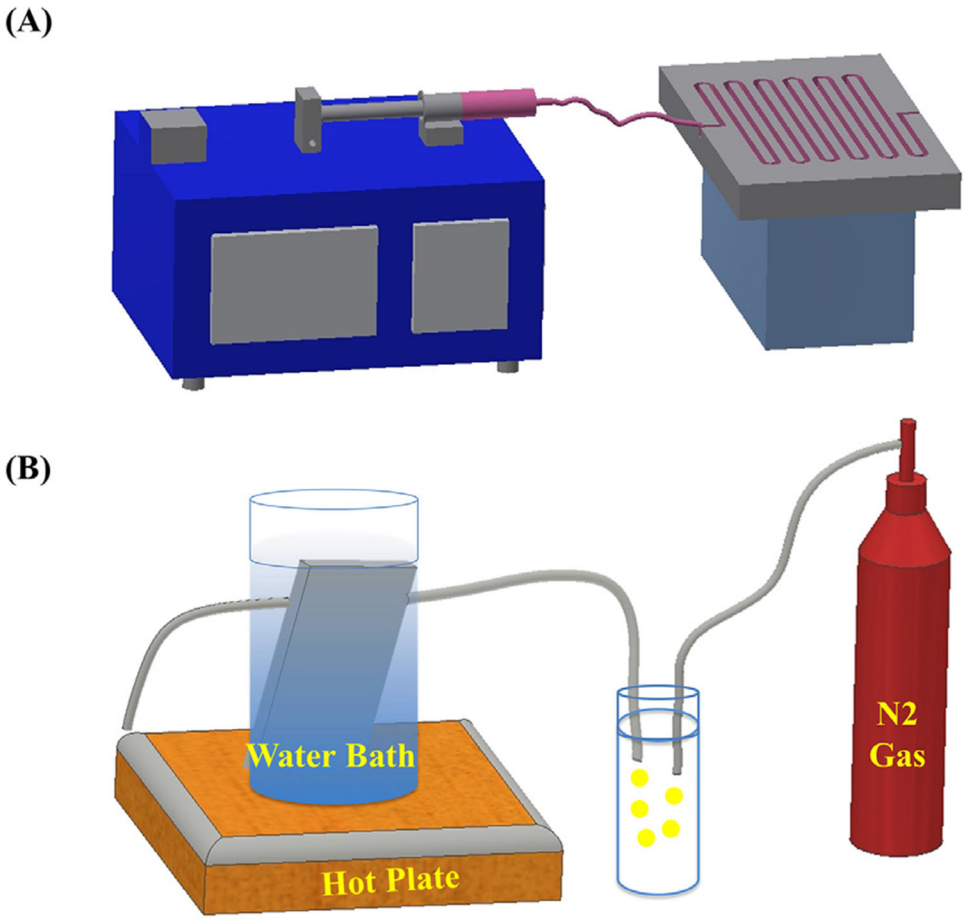

Fig. 1.

(A) Schematic of the coating setup using infusion mode of the syringe pump, process time: 15 min, (B) Schematic of the drying setup including nitrogen purging in the presence of the water bath, process time: 10 min.

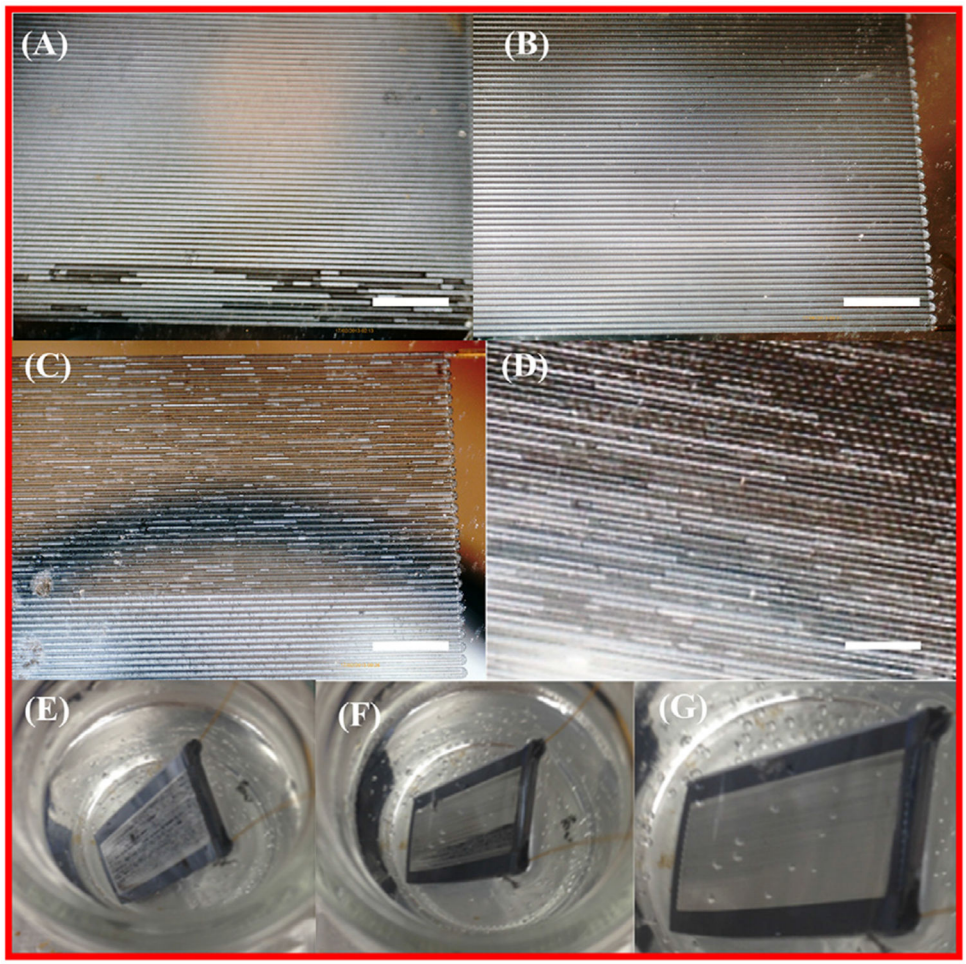

Fig. 2.

Optical images of (A) semi-packed column coated with N_2 purging method and (B) semi-packed column coated with syringe pump. Optical images from drying methods using (C) syringe pump withdraw mode, (D) nitrogen purging, and (E) nitrogen purging with water bath after 1 minute, (F) after 4 minutes, and (G) after 10 minutes. Scale bar: A-C: 4.2 mm, D: 3 mm.

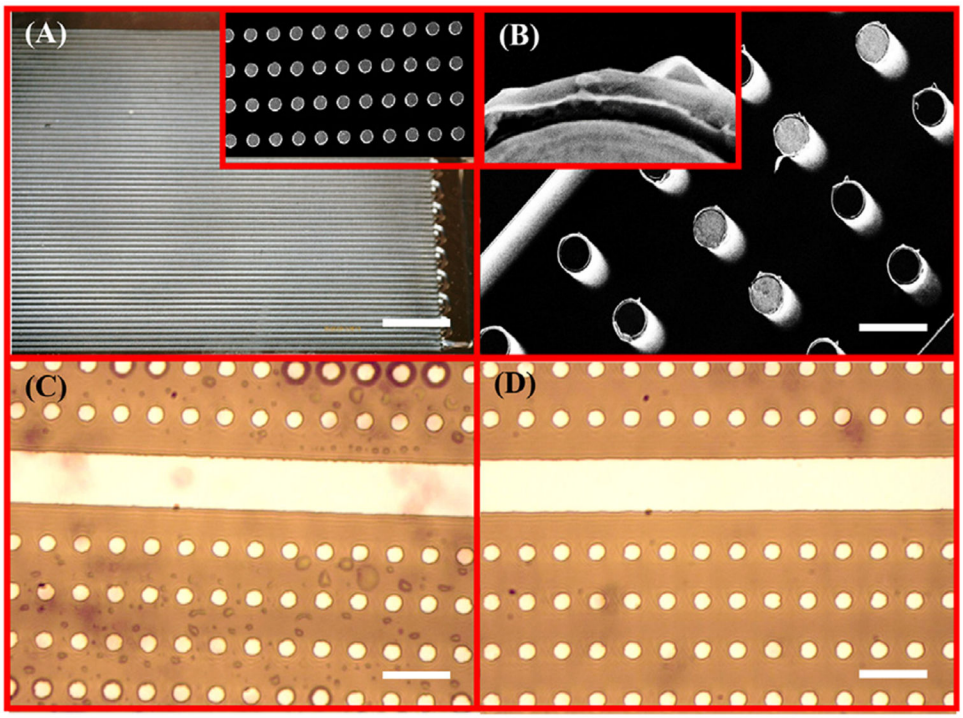

Fig. 3.

(A) column image after oven treatment, inset shows the SEM images of the silicon pillars array, (B) SEM images of the coated silicon pillars with IL1, inset shows magnified image of the stationary phase layer around the pillar, (C) Optical microscope image of pillars before oven thermal treatment, (D) Optical microscope image of the pillars after oven thermal treatment. Scale bars: A: 4.2 mm, B: 40 μm, C, D: 80 μm.

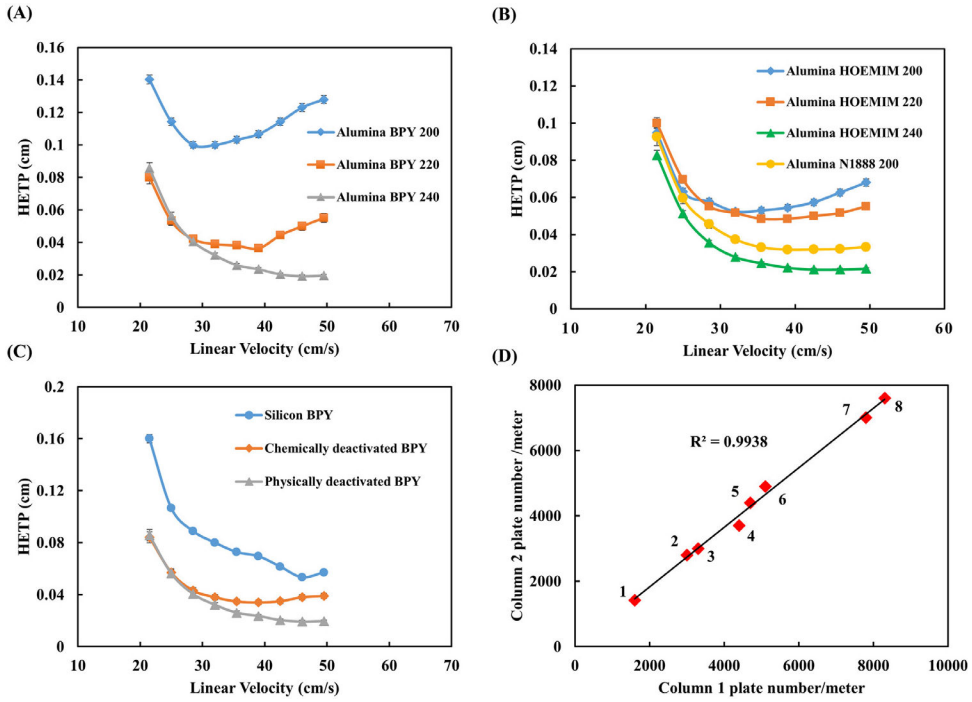

Fig. 4.

Golay plots of the coated columns, (A) Alumina deactivated columns coated with IL1 stationary phase and thermally treated at 200°C, 220°C, and 240°C, (B) Alumina deactivated columns coated with IL2 and IL3 stationary phases, and (C) Silane catalyzed deactivated columns coated with IL1 stationary phase and treated at 240°C, (D) plate number variation for two separate columns of 1: Alumina deactivated column coated with IL1 at 200°C, 2: Silicon column coated with IL1 at 240°C 3: Alumina deactivated column coated with IL2 at 220°C, 4: Alumina deactivated column coated with IL1 at 220°C, 5: Chemically deactivated silicon column with IL1 at 240°C, 6: Alumina deactivated column coated with IL3 at 200°C, 7: Alumina deactivated column coated with IL2 at 240°C, 8: Alumina deactivated column coated with IL1 at 240°C.

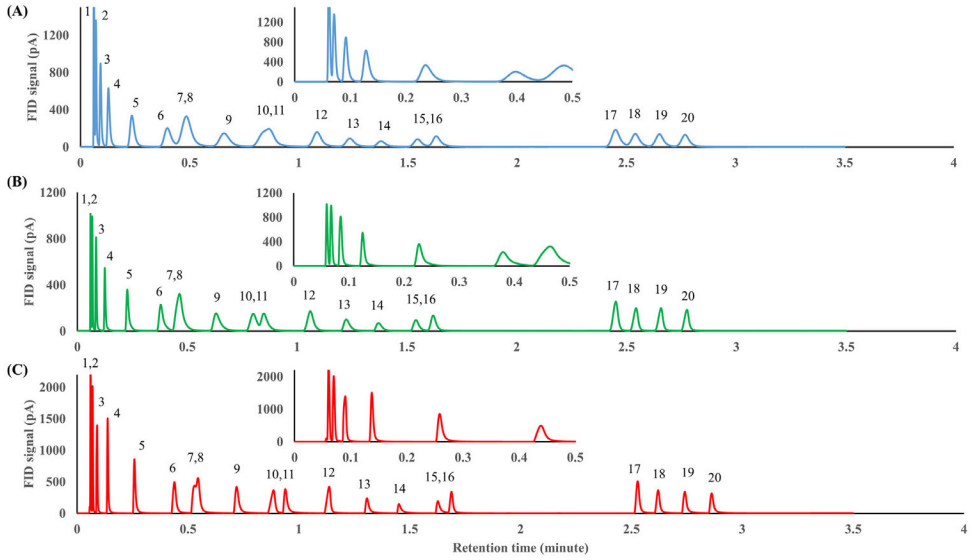

Fig. 5.

Chromatograms showing the separation of the 20 components mixture using IL1 with thermal treatment at (A) 200°C, (B) 220°C, and (C) 240°C. Condition: injection volume 0.1 μL, split ratio 100:1, inlet carrier gas pressure 45 psi, initial oven temperature 30°C held for 0.5 min; ramp rate 40°C/min to 150°C. the retention time of the chemicals is listed in Table 1.

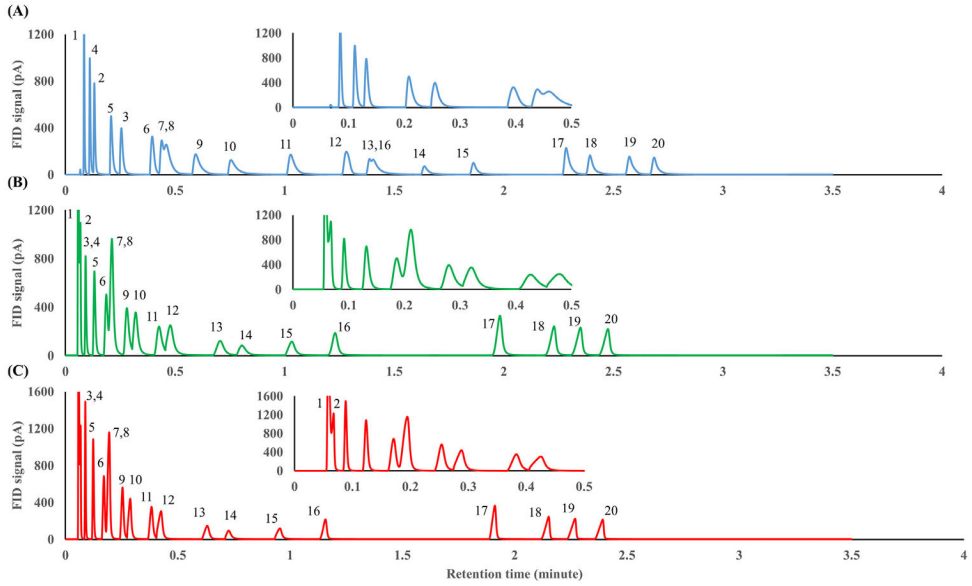

Fig. 6.

Chromatograms showing the separation of the 20 components mixture using (A) IL3 with thermal treatment of 200°C, (B)) IL2 with thermal treatment of 220°C, and (C) IL2 with thermal treatment of 240°C. Condition: injection volume 0.1 μL, split ratio 100:1, inlet carrier gas pressure 45 psi, initial oven temperature 30°C held for 0.5 min; ramp rate 40°C/min to 150°C. The retention time of the chemicals is listed in Table 1.

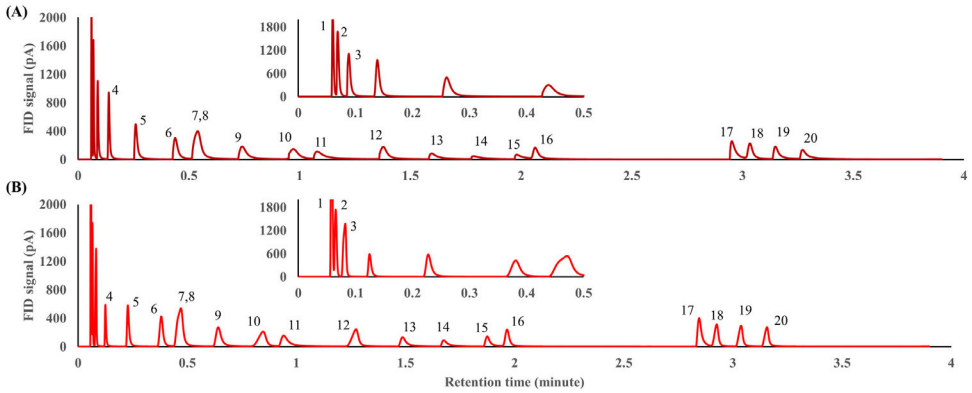

Fig. 7.

Chromatograms showing the separation of the 20 components mixture using IL1 with thermal treatment at 240°C (A) non-deactivated semi-packed column, (B) chemically deactivated semi-packed column. Condition: injection volume 0.1 μL, split ratio 100:1, inlet carrier gas pressure 45 psi, initial oven temperature 30°C held for 0.9 min; ramp rate 40°C/min to 150°C. The retention time of the chemicals is listed in Table 1.

Table 1

The chemical name, number, and boiling point of the 20 components mixture.

Peak number	Chemical name	Boiling point (°C)
1	Heptane	98.4
2	Octane	125.6
3	Nonane	151.0
4	Benzene	80.1
5	Toluene	110.6
6	Ethylbenzene	136.0
7	p-xylene	138.4
8	m-xylene	139.0
9	o-xylene	144.0
10	Isobutylbenzene	173.0
11	Styrene	145.0
12	Butylbenzene	183.3
13	1,2-Dichlorobenzene	180.0
14	2,5-Dichlorotoluene	200.0
15	1,2,4-Trichlorobenzene	214.4
16	Benzyl chloride	179.0
17	Naphthalene	218.0
18	2-Nitrotoluene	222.0
19	3-Nitrotoluene	231.9
20	4-nitrotoluene	238.3

Table 2

Golay plot data.

IL	A	B	C	D
IL1200	0.82	12.05	2.18e-2	1.538e-4
IL1220	0.55	8.54	1.22e-2	7.025e-5
IL1240	0.53	8.49	1.21e-2	9.117e-5
IL2220	0.72	10.69	1.80e-2	1.354e-4
IL2240	0.71	10.48	1.72e-2	1.341e-4
IL3200	0.71	10.65	1.73e-2	1.321e-4

Table 3

Resolution and symmetry of IL1 stationary phase columns (symmetry was reported based on UPS tailing at 5% height of the peak).

Component	Resolution at 200 °C	Tailing at 200 °C	Resolution at 220 °C	Tailing at 220 °C	Resolution at 240 °C	Tailing at 240 °C
Naphthalene	12.11	1.17	19.59	1.07	33.12	1.46
2-nitrotoluene	1.32	1.30	2.28	1.05	3.47	1.47
3-nitrotoluene	1.62	1.15	2.94	1.03	4.51	1.85
4-nitrotoluene	1.75	1.21	3.12	1.11	4.50	1.95

Table 4

Resolution and symmetry of IL2, IL3 stationary phase columns (symmetry was reported based on UPS tailing at 5% height of the peak).

Component number	Resolution IL3 at 200 °C	Tailing IL3 at 200 °C	Resolution IL2 at 220 °C	Tailing IL2 at 220 °C	Resolution IL2 at 240 °C	Tailing IL2 at 240 °C
Naphthalene	11.04	2.16	16.68	1.09	24.10	0.78
2-nitrotoluene	2.82	2.30	5.47	0.92	7.21	0.70
3-nitrotoluene	4.52	1.94	2.61	0.87	3.25	0.69
4-nitrotoluene	2.82	2.37	2.68	0.87	3.29	0.69

Table 5

stability data for 100 experimental chromatograms.

Column type	Height (pA)	Width (Second)	Symmetry	Time (Second)
IL1 mean	195.7	2.2	1.0	53.5
IL1 RSD%	2.1	0.1	0.1	0.02
IL2 mean	387	1.1	1.0	25.1
IL2 RSD%	4.5	0.5	2.0	0.1
IL3 mean	225.7	1.6	0.8	39.4
IL3 RSD%	4.5	2.3	0.3	0.1

RSD: relative standard deviation.